Evaluation of Different Approaches for Transmission Tomography in Ultrasound Computer Tomography

Nicole V. Ruiter, Tim O. Müller, Rainer Stotzka and Hartmut Gemmeke

Forschungszentrum Karlsruhe, Institute for Data Processing and Electronics
Email: nicole.ruiter@ipe.fzk.de

Abstract. An evaluation of standard methods for reconstruction of sound velocity maps for Ultrasound Computer Tomography (USCT) is presented. Different approaches for detection of transmission signals and sound velocity reconstruction are compared using a simulated and a measured data set. The sound velocity map of the measured object could be reconstructed with 3.6 m/s difference between the reconstructed and the real sound velocities, which is feasible for improvement of USCT reflection and scattering images. But the images of the reconstructed velocity maps are blurry and full of artifacts, so that they are at this state of the work only of limited use for diagnostic purposes.

1 Introduction

With conventional ultrasound scanners for breast examination the measurement of the diagnostically relevant sound velocity [1] is not feasible. Our new technique, Ultrasound Computer Tomography (USCT), records scattered, reflected and transmitted ultrasound signals in 3D, resulting from the emissions of non focused spherical pressure wave. In contrast to conventional ultrasound scanners, the sender and emitter positions are separated and the transducers are arranged in a fixed cylinder geometry. In addition to high–resolution reflection and scattering images, sound velocity maps of the breast tissue can be reconstructed via transmission tomography. These maps can be used either as additional diagnostic information or to improve the reflection images. A sketch of the geometry of an experimental one–layer acquisition system and an example ultrasound signal is given in Fig. 1.

In transmission tomography the transmitted signal is used for reconstruction, i.e. the ultrasound pulse travelling directly from emitter to receiver. The arrival time of the ultrasound pulse is called the time–of–flight and is used together with the distance between emitter and receiver to calculate the average sound velocity. Two methods for robust detection of the time–of–flight and three standard approaches for back–projection of the sound velocities are compared in this paper in order to find the method best suited for USCT. In this evaluation only methods assuming linear propagation of the transmitted signal, i.e. neglecting refraction effects, are considered.

Fig. 1. Architecture of the USCT system for one–layer acquisition. A ring of ultrasound transducers encloses the object (left). One transducer emits a short ultrasound pulse, all other transducers receive simultaneously. The A–scan at the right hand side shows the transmitted, reflected and scattered signals.

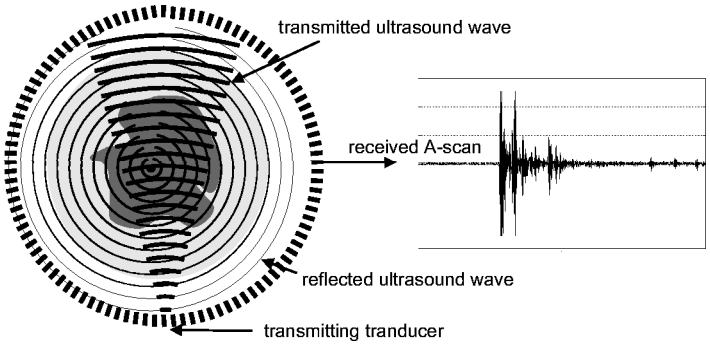

State of the Art. In literature two different approaches for recording the transmission have been described. Firstly, a metallic reflector was used together with a conventional ultrasound scanner, reflecting the transmitted signal like a mirror [1]. Secondly, the transmitted signal is measured using separate emitter and receiver positions, as given in USCT. This has first been proposed by Greenleaf at al [2] and is applied in different ultrasound acquisition systems, e.g. as spiral CT with two parallel conventional ultrasound scanners [3].

Many different approaches for reconstruction of sound velocity maps have been proposed in literature. Simple back–projection [4], where the projected beams are smeared back into the image, ignoring the mathematical correct filter, the inverse Radon transformation [5] including the filtering, or application specific methods, e.g. [6], can be distinguished. Most available algorithms consider parallel beam geometries as used in X–ray CT.

2 Methodology

Detection of the Transmission Signal. To image an object, all emitters sequentially send a short ultrasound pulse, in this application three approximately gaussian weighted sinus waves at 3 MHz. The recorded signals are called A–scans, i.e. the pressure variation of the ultrasonic field over time at each receiver position. The signal traveling the shortest distance, i.e. the first pulse, is the transmission signal. In order to reconstruct a sound velocity map the average sound velocity for each emitter and receiver position has to be obtained, calculated by dividing the distance between emitter and receiver by the time–of–flight.

The received A–scans are noisy and due to absorption the amplitude of the transmission signal can be very small. For such signals with low signal–to–noise ratio simple thresholding cannot be applied. Two methods, each applying knowledge about the transmitted pulse, are considered. First, auto–correlation at the

mean frequency of the submitted pulse is applied. The first local maximum of the auto–correlation gives the time–of–flight. Second, spiking deconvolution followed by thresholding is evaluated. The pulse response of the system for the Wiener filtering [7] is derived from the transmission pulse obtained with our USCT only filled with water. As threshold the maximum value of the noise at the beginning of the signal is used.

A general limit to the accuracy of the detection is given by the discretization of the A–scan, here sampling rates of 10 and 50 MHz were considered. Additional error sources are the limited accuracy of the known distance between emitter and receiver with an uncertainty of approx. 0.1 mm and the corruption of the time–of–flight detection due to noise.

Reconstruction of the Sound Velocity Map. As given in Fig. 1 the geometry of one emitter and all other transducers receiving is an equiangular fan beam geometry. For the evaluation of image reconstruction in USCT the following methods are applied: First, an unfiltered fan beam back–projection is applied using two slightly different methods. In one case each measured point contributes to a line between emitter and receiver and in the other case each pixel is built by calculating all possible intersecting lines of emitters and receivers. Second, the mathematically correct inverse Radon transformation for equiangular fan beam projections is applied [8].

A general limit to the accuracy of the reconstructed sound velocity maps is given by the limited number of 100 recorded projections and the discretization of the projections by 1440 receiving points. Additional sources of error are non–linear propagation of sound due to refraction and the limited accuracy of the geometry.

Analyzed Data. The performance of the combined detection and reconstruction methods is tested on two data sets. First, a data set of simulated A–scans was generated ('simulated'). A circular object (sound velocity 1500 m/s, diameter 7 cm) embedded in water (1485 m/s at 21°C) was simulated by placing a source pulse of a wave train of three sinus waves at 3 MHz at the appropriate time–of–flight in the A–scans. Attenuation, reflection, scattering, refraction and noise were neglected.

Second, a measured data set was obtained. The A–scans of the gelatin phantom ('gelatine') were recorded with the experimental one–layer acquisition system. The phantom consists of gelatin in a plastic container (square box with approx. 7 cm diameter), with an average sound velocity of approx. 1530 m/s. For the measurement it was embedded in water. In this case non–linear propagation, noise and attenuation are included in the A–scans. Additionally to the attenuation of the gelatin, the lid of the plastic container caused strong attenuation at certain angles, reducing the amplitude of some transmission signals to the level of the noise.

Table 1. The mean velocity differences in [m/s] of the reconstructed sound velocity maps and the real mean sound velocities of the simulated data (Simulated) and the gelatin phantom (Gelatin) are displayed for deconvolution (Dec) and auto–correlation (Aut) detection. The sound velocity maps were reconstructed using unfiltered point based (Point), unfiltered pixel based (Pixel) and filtered inverse Radon transform for fan beam geometry (Radon) algorithms.

	Point Dec	Point Aut	Pixel Dec	Pixel Aut	Radon Dec	Radon Aut
Simulated, 50 MHz	4.4	3.8	4.7	4.0	1.8	2.1
Simulated, 10 MHz	5.3	11.9	5.6	15.1	1.8	10.7
Gelatin, 50 MHz	28.0	15.6	25.1	18.4	40.3	7.9
Gelatin, 10 MHz	15.4	20.7	15.7	21.9	3.6	15.4

3 Results

Measurement of the Detection Quality. For the simulated data set a deviation of the time–of–flight detected by auto–correlation was found as average 44.9 μs and 4.5 μs (maximum 71.1 μs and 7.1 μs) at 10 MHz and 50 MHz sampling, respectively. For detection by deconvolution the average distances were 0.1 μs and 0.02 μs (maximum 0.1 μs and 0.02 μs) for 10 MHz and 50 MHz sampling, respectively. For the gelatin phantom the percentage of undetected time–of–flight signals is at 10 MHz 7.1% for auto–correlation and 14.4% for deconvolution. With the higher background noise at 50 MHz, auto–correlation detected the time–of–flight for each A–scan, but not all of them were meaningful as auto–correlation tends to detect random signals, when the transmission signal is low. Deconvolution detected only approx. 50% of the time–of–flight positions, due to the noise sensitivity of this method.

Results of the Reconstruction of the Sound Velocity Maps. For all analyzed data sets the mean distances between the reconstructed sound velocity maps and the real sound velocities for point based ('Point') and pixel based ('Pixel') unfiltered back–projection and the filtered inverse radon transform for fan beam geometry ('Radon') are given in Table 1. The reference velocity maps were created including the sound velocity of the surrounding water and the velocity of the object. The velocity maps were reconstructed with 128^2 pixel, corresponding to a pixel width of 1 mm.

4 Discussion and Conclusion

The best results for the gelatine phantom were obtained with deconvolution based detection of the transmission signal and reconstruction using filtered inverse Radon transform for fan beam geometry for sampling at 10 MHz. The high deviation of the deconvolution results for the 50 MHz gelatin phantom are due to the additional high frequency noise at this sampling frequency. In general the

differences are on the one hand due to variance of the time–of–flight detection in noisy data and errors in the measured distance between emitter and receiver, on the other hand due to the assumption of linear propagation of ultrasound through tissue.

The velocity differences between the reconstructed and real sound velocities of the gelatin phantom are small enough to be feasible for improvement of the reflection images by including the sound velocities in the reconstruction. In contrast to that the reconstructed images are blurry and contain many artifacts and are therefore not applicable for diagnostic purposes. This is due to the fact that in our experimental USCT setup 100 different emitter positions were recorded with 1400 receiver positions each, therefore the recommended identity of the number of sending positions and receiving positions [8] is violated by our system architecture.

The next steps will be: Construction of a phantom with different sized structures and small sound velocity differences to investigate the image quality of the velocity maps further. Correction techniques will be applied to cope for the non–linear ultrasound propagation. Additionally, the reconstruction technique can be easily modified to calculate absorption images as well. For the next generation USCT system, where volume data is acquired instead of slice data, the transmission tomography algorithms have to be extended to 3D reconstruction.

References

1. Richter K. Clinical Amplitude / Velocity Reconstruction Imaging (CARI) – a New Sonographic Method for Detecting Breast Lesions. Br J Radiol 1995;68:375–385.
2. Greenleaf JF, Johnson SA, et al. Algebraic Reconstruction of Spatial Distributions of Acoustic Velocities in Tissue from their Time–Of–Flight Profiles. Acoustic Holography 1975;7:71–90.
3. Ashfaq M, Ermert H. Ultrasound Spiral CT for the Female Breast – First Phantom Imaging Results. Biomed Tech (Berl) 2001;46(1):70–71.
4. Deck T, Müller TO, Stotzka R. Rekonstruktion von Geschwindigkeits– und Absorptionsbildern eines Ultraschall–Computertomographen. In: Procs BVM; 2003. p. 136–140.
5. Jago JR, Whittingham TA. Experimental Studies in Transmission Ultrasound Computed Tomography. Phys Med Biol 1991;36(11):1515–1527.
6. Nguyen MT, Bessmer H, et al. Improvements in Ultrasound Transmission Computed Tomography. In: European Conference on Engineering and Medicine; 1993.
7. Jensen JA, Mathorne J, et al. DECONVOLUTION OF IN–VIVO ULTRASOUND B–MODE IMAGES. Ultrason Imaging 1993;15:122–133.
8. Kak AC, Slaney M. Principles of Computerized Tomographic Imaging. IEEE Press; 1987.